

# Pyridoxamine alleviates mechanical allodynia by suppressing the spinal receptor for advanced glycation end product-nuclear factor- $\kappa$ B/extracellular signal-regulated kinase signaling pathway in diabetic rats

Xin Zhang<sup>1,2</sup> , Li Xu<sup>1</sup>, Weiyun Chen<sup>1</sup>, Xuerong Yu<sup>1</sup>, Le Shen<sup>1</sup> , and Yuguang Huang<sup>1</sup>

Molecular Pain  
Volume 16: 1–12  
© The Author(s) 2020  
Article reuse guidelines:  
sagepub.com/journals-permissions  
DOI: 10.1177/1744806920917251  
journals.sagepub.com/home/mpx



## Abstract

Diabetic neuropathic pain is a common complication of diabetes mellitus and requires a substantial amount of societal resources. Pyridoxamine is an inhibitor of advanced glycation and lipoxidation end products. Several animal and clinical studies have confirmed that pyridoxamine can inhibit a range of pathological changes in diabetes-induced organ injury and alleviate certain kinds of neuropathic pain. However, no studies have attempted to explore the effects of pyridoxamine on diabetic neuropathic pain. We conducted animal experiments to examine whether pyridoxamine could alleviate diabetic neuropathic pain and to explore the mechanism underlying these effects. Adult male Sprague Dawley rats were randomly assigned to the normal + sterile water group, diabetic + sterile water group, diabetic + pyridoxamine<sub>100</sub> group, diabetic + pyridoxamine<sub>200</sub> group, diabetic + pyridoxamine<sub>400</sub> group, or normal + pyridoxamine group. The rats in the diabetic + pyridoxamine<sub>100</sub>, diabetic + pyridoxamine<sub>200</sub>, diabetic + pyridoxamine<sub>400</sub>, and normal + pyridoxamine groups received pyridoxamine at dosages of 100 mg/kg/day, 200 mg/kg/day, 400 mg/kg/day, and 400 mg/kg/day, respectively, via intragastric administration. The rats in the other groups received water daily. Pyridoxamine alleviated diabetic neuropathic pain at least partially by suppressing the activity of the spinal receptor for advanced glycation end products-nuclear factor- $\kappa$ B/extracellular signal-regulated kinase signaling pathway; additionally, pyridoxamine decreased advanced glycation end product-modified low-density lipoprotein, oxidized low-density lipoprotein, and interleukin-1 $\beta$  levels in the serum. The immunofluorescence staining results revealed that most phosphorylated nuclear factor- $\kappa$ B was localized to neuronal cells and not to microglia or astrocytes; this pattern may be associated with the upregulated expression of pain-related proteins. The abovementioned results indicate that pyridoxamine is a promising choice for the clinical treatment of diabetic neuropathic pain. Further investigations need to be carried out to confirm the benefits of pyridoxamine.

## Keywords

Diabetic neuropathic pain, pyridoxamine, receptor for advanced glycation end products, nuclear factor- $\kappa$ B, extracellular signal-regulated kinase

Date received: 16 February 2019; revised: 22 February 2020; accepted: 26 February 2020

<sup>1</sup>Department of Anesthesiology, Peking Union Medical College Hospital, Chinese Academy of Medical Sciences, Peking Union Medical College, China

<sup>2</sup>Department of Anesthesiology, National Cancer Center/National Clinical Research Center for Cancer/Cancer Hospital, Chinese Academy of Medical Sciences, Peking Union Medical College, China

## Corresponding Authors:

Le Shen, Department of Anesthesiology, Peking Union Medical College Hospital, Chinese Academy of Medical Sciences, Peking Union Medical College, Beijing, China.

Email: pumchshenle@aliyun.com

Yuguang Huang, Department of Anesthesiology, Peking Union Medical College Hospital, Chinese Academy of Medical Sciences, Peking Union Medical College, Beijing, China.

Email: garybeijing@163.com



## Introduction

The global epidemic of diabetes mellitus (DM) imposes tremendous burdens on patients and society at large. Diabetic neuropathic pain (DNP) is a common complication of DM that occurs in 11% to 21% of DM patients,<sup>1</sup> producing symptoms of numbness, pain, and paresthesia. DNP treatment consists of two major methods: glycemic control and interventions targeting pathophysiological mechanisms.<sup>2,3</sup>

High blood glucose (BG) levels create an appropriate environment for the occurrence of some chemical modifications—for example, glycooxidation and advanced glycosylation. Advanced glycosylation occurs through a series of chemical reactions. In the early stage of the process, glucose forms reversible advanced glycosylation products with proteins. If these proteins have sufficiently long half-lives, the early advanced glycosylation products will transform into more stable products called advanced glycation end products (AGEs).<sup>4</sup> The advanced glycosylation of proteins is believed to be an important cause of diabetic complications. The formation of endogenous AGEs can lead to the activation of several inflammatory signaling pathways.<sup>5</sup> Brederson et al.<sup>6</sup> found that a monoclonal antibody against the receptor for advanced glycation end products (RAGE) attenuated inflammatory and neuropathic pain in mice, indicating that the binding of AGEs to RAGE may be associated with neuropathic pain.

Approaches to the treatment of DNP are multimodal and multidisciplinary.<sup>7</sup> Anticonvulsants, antidepressants, and opioids are the primary pharmacological choices for DNP treatment. Pyridoxamine is a derivative of vitamin B6 and plays important roles in whole-body metabolism.<sup>8</sup> Pyridoxamine is also an inhibitor of AGEs and advanced lipoxidation end products (ALEs). In several studies, pyridoxamine treatment significantly improved the kidney function of diabetic rats,<sup>9</sup> reverted the methylglyoxal-induced impairment of survival pathways during heart ischemia,<sup>10</sup> and provided protection in animal models of diabetic retinopathy.<sup>11</sup> Yu et al.<sup>12</sup> reported that systematic administration of B vitamins (B<sub>1</sub>, B<sub>6</sub>, and B<sub>12</sub>) may effectively reduce neuropathic pain after spinal cord ischemia/reperfusion injury, and a randomized, double-blind, placebo-controlled trial showed that an AGE inhibitor (benfotiamine [50 mg] + pyridoxamine [50 mg] + methylcobalamin [500 µg]) decreased pain and inflammation in osteoarthritis patients.<sup>13</sup> The results of these studies indicate that pyridoxamine may be valuable in the treatment of pain. However, no studies have investigated pyridoxamine as a treatment for DNP. Therefore, we designed a study to examine whether pyridoxamine could alleviate DNP and explored the mechanism underlying these effects.

## Materials and Methods

### Animals

Adult male Sprague Dawley rats (220–250 g, 6–7 weeks) were used in this study. The study protocol was approved by the Ethical Committee for Animal Experimentation of the Peking Union Medical College Hospital. Rats were housed at 23 ± 1°C under a 12-h light/dark cycle for 3 to 5 days before being used in the experimental procedures. To investigate the dose-dependent efficacy of pyridoxamine, we randomly assigned the animals to the normal + sterile water (NW) group, diabetic + sterile water (DW) group, diabetic + pyridoxamine<sub>100</sub> (DP<sub>100</sub>) group, diabetic + pyridoxamine<sub>200</sub> (DP<sub>200</sub>) group, diabetic + pyridoxamine<sub>400</sub> (DP<sub>400</sub>) group, or normal + pyridoxamine (NP) group.

### Model of DNP

The animals were fasted for 12 h before the induction of diabetes. Each rat in the DW and DP groups received a single intraperitoneal injection of streptozotocin (STZ) (Sigma–Aldrich, St. Louis, USA) at a dose of 60 mg/kg body weight. The STZ was freshly dissolved in citrate buffer (pH = 4.5) at a concentration of 1%. The rats in the NW and NP groups were injected with citrate buffer alone. Three days after the STZ injection, diabetes was confirmed if the BG concentration was >16.7 mmol/L, as determined using a glucometer (Sinocare, Changsha, China). The threshold for the diabetic BG level was determined by referring to research articles related to DNP.<sup>14–16</sup> The rats in the DP<sub>100</sub>, DP<sub>200</sub>, DP<sub>400</sub>, and NP groups received pyridoxamine at dosages of 100, 200, 400, and 400 mg/kg/day, respectively, by intragastric administration. The rats in the other groups received water every day. The experimental protocol is summarized in Figure 1.

### Behavioral testing

The paw withdrawal mechanical threshold (PWMT) was measured using an electronic von Frey esthesiometer (IITC Life Science, CA, USA) consisting of a hand-held force transducer and a fixed tungsten wire tip

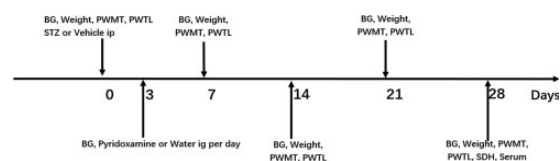


**Figure 1.** Experimental protocol.

BG: blood glucose; PWMT: paw withdrawal mechanical threshold; PWTL: paw withdrawal thermal latency; STZ: streptozotocin; ig: intragastric; SDH: spinal dorsal horn.

with a diameter of 200  $\mu\text{m}$ . Each rat was placed in a chamber (11  $\times$  21  $\times$  25 cm) with a wire grid floor for at least 30 min. The researcher applied the tip vertically to the plantar surface of the hind paw with a gradually increasing force until paw withdrawal was elicited. The maximum force was automatically recorded. The average of three successful readings was used as the PWMT.

A radiant thermal stimulator (BME-410A, China) was used to assess thermal hyperalgesia. Each rat was placed in a chamber (11  $\times$  21  $\times$  25 cm) on a 2-mm thick glass platform for at least 30 min before testing. The researcher focused a radiant heat source located below the glass on the plantar surface of the hind paw. The time to the end point of lifting or licking of the hind paw was recorded, and the average of three successful readings was used as the paw withdrawal thermal latency (PWTL).

### Western blot analysis

L3-5 spinal dorsal horns (SDHs) were harvested from rats anesthetized with sodium pentobarbital (60 mg/kg body weight) and then homogenized in RIPA buffer (CWBio, Beijing, China) supplemented with protease inhibitors and phosphatase inhibitors. After centrifugation (12,000  $\times g$  for 15 min), the supernatants were collected and denatured in SDS-polyacrylamide gel electrophoresis (SDS-PAGE) loading buffer (Applygen, Beijing, China) for 10 min at 100°C. Tissue extracts were electrophoresed on 10% SDS-PAGE gels and subsequently transferred to polyvinylidene difluoride membranes (Millipore, Billerica, USA). The membranes were blocked with 5% nonfat dry milk or 5% bovine serum albumin (BSA) in Tris-buffered saline with Tween 20 for 1 h before incubation with primary antibodies at 4°C overnight. The following primary antibodies were applied: anti-RAGE (Bioss, Beijing, China), anti-nuclear factor (NF)- $\kappa\text{B}$  (Cell Signaling Technology (CST), Boston, USA), anti-phosphorylated (p-) NF- $\kappa\text{B}$  (CST, Boston, USA), anti-extracellular signal-regulated kinase (ERK; CST, Boston, USA), anti-p-ERK (CST, Boston, USA), anti-p38 (CST, Boston, USA), anti-p-p38 (CST, Boston, USA), anti-c-Jun N-terminal kinase (JNK; CST, Boston, USA), anti-p-JNK (CST, Boston, USA), and anti- $\beta$ -actin (ZSGB-BIO, Beijing, China). The membranes were washed (three times for 10 min each) and incubated with the corresponding secondary antibodies for 1 h at room temperature. Signals were detected by a SuperEnhanced chemiluminescence detection kit (Applygen, Beijing, China), and protein bands were visualized with a Tanon 5800 multichannel chemiluminescence imaging system (Tanon, Shanghai, China). ImageJ software (version 1.45s; NIH, Bethesda, USA) was used to quantitatively analyze the band densities.

### Immunofluorescence staining

Animals were anesthetized with sodium pentobarbital (60 mg/kg body weight) and perfused with phosphate-buffered saline (PBS) followed by fresh 4% paraformaldehyde. L3-5 SDHs were collected from rats, fixed in 4% paraformaldehyde overnight and cryopreserved in 30% sucrose at 4°C overnight. Tissues were mounted and sectioned on a cryostat at a thickness of 12  $\mu\text{m}$ . Tissue sections were permeabilized with 0.3% Triton X-100 (Amresco, Solon, USA) in PBS for 15 min, followed by antigen retrieval with Quick Antigen Retrieval Solution for Frozen Sections (Beyotime, Jiangsu, China). Then, the sections were incubated with 3% BSA for 1 h at room temperature and then with primary antibodies overnight at 4°C. The following primary antibodies were used: anti-gial fibrillary acidic protein (GFAP; Abcam, Cambridge, UK), anti-ionized calcium binding adaptor molecule 1 (IBA1; Abcam, Cambridge, UK), anti-NeuN (Abcam, Cambridge, UK), anti-p-NF- $\kappa\text{B}$  (Abcam, Cambridge, UK) and anti-RAGE (Abcam, Cambridge, UK). The tissue sections were washed three times and incubated with the appropriate secondary antibodies for 1 h at room temperature. After the slides were washed in PBS, coverslips were applied with mounting medium with DAPI (ZSGB-BIO, Beijing, China). The sections were examined on an Olympus fluorescence microscope (Olympus, Tokyo, Japan).

### Enzyme-linked immunosorbent assay (ELISA)

The levels of interleukin-1 $\beta$  (IL-1 $\beta$ ) and tumor necrosis factor- $\alpha$  (TNF- $\alpha$ ) in the SDH and the levels of oxidized low-density lipoprotein (ox-LDL), AGE-modified low-density lipoprotein (AGE-LDL), and IL-1 $\beta$  in the serum were quantified using ELISA kits according to the manufacturer's instructions. The ox-LDL and AGE-LDL ELISA kits were purchased from Xinqidi Biological Technology (Wuhan, China). The IL-1 $\beta$  and TNF- $\alpha$  ELISA kits were purchased from Shanghai Jianglai Biotech (Shanghai, China). Serum samples were collected four weeks after STZ injection. Tissue cytokine concentrations were expressed as pg protein/mL sample.

### Statistical analysis

Data are presented as the mean  $\pm$  standard deviation (SD). The western blot and ELISA data were analyzed using one-way analysis of variance (ANOVA) with Dunnett's test. Two-way ANOVA was used to analyze the BG, weight, and mechanical pain threshold data. Fisher's exact test was used to analyze the immunofluorescence staining data.  $P < 0.05$  was considered statistically significant.

## Results

### Effects of pyridoxamine on BG, weight, and neuropathic pain

Before the STZ-mediated induction of diabetes, the BG level and weight of the rats in each group were normal and not significantly different among the groups. One week after STZ injection, however, the BG levels in the DW, DP<sub>100</sub>, DP<sub>200</sub>, and DP<sub>400</sub> groups were significantly higher than those in the NW group (Figure 2(a)). The rate of weight gain in the DW, DP<sub>100</sub>, DP<sub>200</sub>, and DP<sub>400</sub> groups was much slower than that in the NW group, and the mean weights of rats in the DW, DP<sub>100</sub>, DP<sub>200</sub>, and DP<sub>400</sub> groups were significantly lower than those of rats in the NW group one week after STZ injection (Figure 2(b)).

The baseline PWMT was similar among the six groups. Compared with rats in the NW group, rats in the DW group exhibited a decrease in PWMT one week after STZ injection, and the difference between these groups was statistically significant at two weeks. The administration of pyridoxamine at dosages of 200 mg/kg/day and 400 mg/kg/day significantly inhibited the decrease in PWMT in diabetic rats, and these effects lasted for at least four weeks; however, no significant differences were observed between the DP<sub>200</sub> and DP<sub>400</sub> groups. The administration of pyridoxamine at a dosage of 100 mg/kg/day did not inhibit the decrease

in PWMT in diabetic rats. No significant differences were found between the NP group and the NW group during the four weeks (Figure 2(c)).

Compared to the NW group, the DW group exhibited a mild decrease in PWTL two weeks after STZ injection; however, the difference was not significant (Figure 2(d)).

### Pyridoxamine inhibited RAGE/NF- $\kappa$ B expression in the SDH of diabetic rats

RAGE is involved in the pathophysiological changes in many diabetic complications, such as diabetes-associated osteoporosis,<sup>17</sup> diabetic nephropathy,<sup>18</sup> and vascular calcification.<sup>19</sup> Because pyridoxamine did not affect baseline pain sensitivity in nondiabetic animals and because the optimal dosage was 200 mg/kg/day, we investigated the changes in RAGE expression in the SDH of rats in the NW, DW, and DP<sub>200</sub> groups via western blot analysis. RAGE expression was significantly upregulated in the DW group compared with that in the NW group, and pyridoxamine inhibited RAGE expression in the SDH of diabetic rats (Figure 3(a)).

NF- $\kappa$ B is activated when AGEs (and other ligands) bind to RAGE.<sup>20</sup> Therefore, total NF- $\kappa$ B and p-NF- $\kappa$ B levels were measured via western blot analysis. Diabetes significantly increased the phosphorylation of NF- $\kappa$ B in the DW group compared to that in the NW group, and the treatment of diabetic rats with pyridoxamine significantly attenuated this increase (Figure 3(b)).

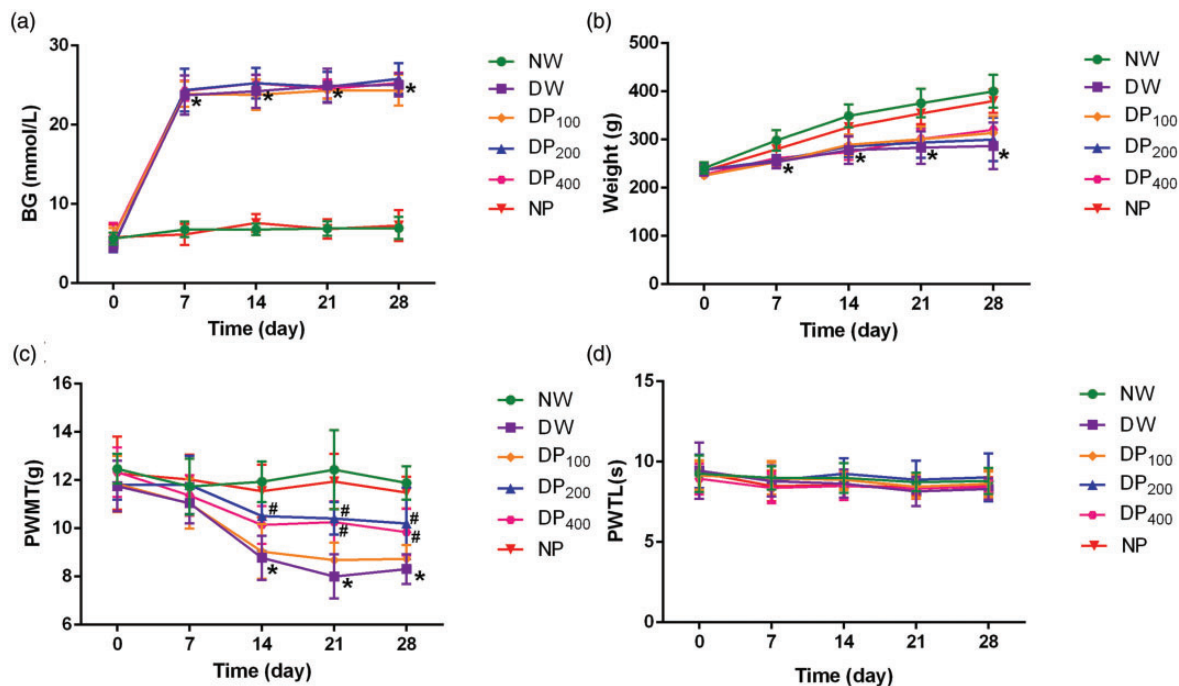


**Figure 2.** Changes in baseline characteristics in the six groups of rats. (a) BG levels in the six groups were measured over the 28-day observation period. (b) Weight changes in the six groups during the observation period. (c) Changes in the PWMT values in the six groups. (d) Changes in the PWTL values in the six groups. \* $P < 0.05$  vs. the NW group, # $P < 0.05$  vs. the DW group.  $N = 8$  in all the groups.



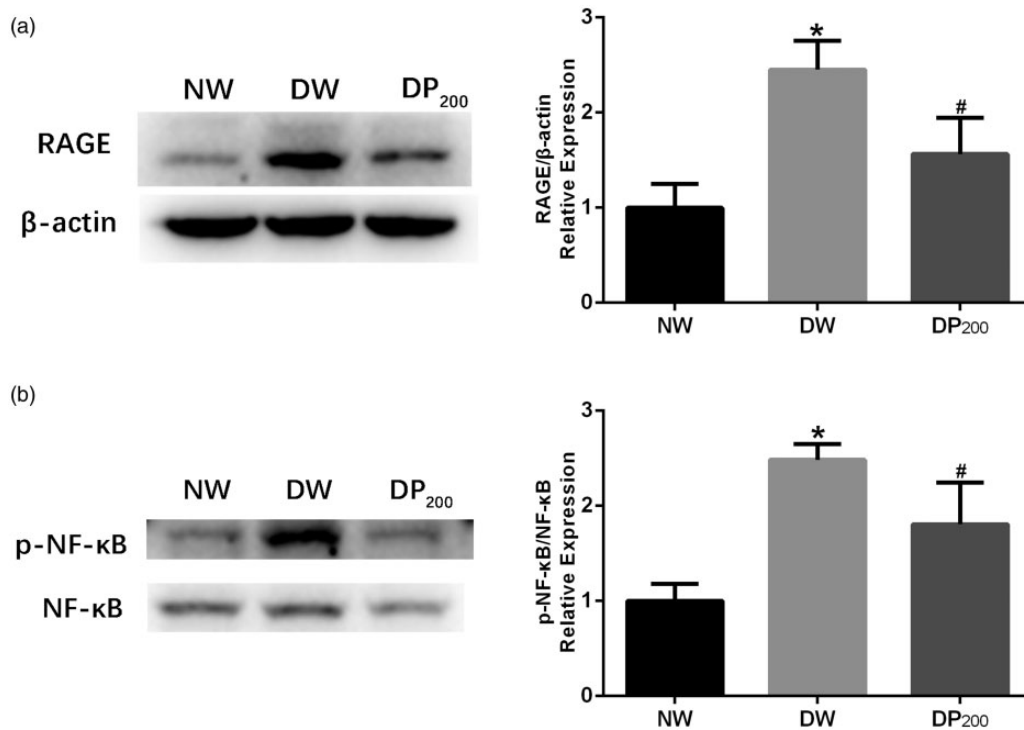


**Figure 3.** Expression of RAGE/NF- $\kappa$ B in the three groups. (a) Representative western blots and statistical graphs showing the RAGE protein levels in the SDH of rats in the three groups. (b) Representative western blots and statistical graphs showing the expression of p-NF- $\kappa$ B in the SDH of rats in the three groups. The band densities were normalized to those of the NW group. \* $P < 0.05$  vs. the NW group, # $P < 0.05$  vs. the DW group.  $N = 5$  per group.

#### *IL-1 $\beta$ and TNF- $\alpha$ expression was not upregulated in the SDH of diabetic rats*

The expression of IL-1 $\beta$  and TNF- $\alpha$  is upregulated when NF- $\kappa$ B is activated.<sup>21,22</sup> Therefore, we measured the concentrations of IL-1 $\beta$  and TNF- $\alpha$  in the SDH of rats in the three groups using ELISA kits. However, no differences were found among the three groups (Figure 4).

#### *Phosphorylated NF- $\kappa$ B and RAGE were mainly localized in neuronal cells in the SDH of diabetic rats*

We used immunofluorescence staining to identify the cell type in which NF- $\kappa$ B was phosphorylated. The microglial marker IBA1 showed almost no colocalization with p-NF- $\kappa$ B, and the astrocyte marker GFAP was not colocalized with p-NF- $\kappa$ B. In contrast, the neuronal marker NeuN displayed the best colocalization with p-NF- $\kappa$ B (Figure 5). Our experiments revealed that most p-NF- $\kappa$ B was localized in neuronal cells and not in microglia or astrocytes.

In addition, we explored the subcellular distribution of RAGE and found results similar to those obtained for p-NF- $\kappa$ B (Figure 6).

#### *Pyridoxamine suppressed ERK phosphorylation in the SDH of diabetic rats*

Mitogen-activated protein kinases (MAPKs) are activated in the SDH of diabetic rats and contribute to diabetic mechanical hyperalgesia.<sup>23</sup> We therefore examined the phosphorylation status of ERK, p38, and JNK in the SDH of rats in the NW, DW, and DP<sub>200</sub> groups. Diabetes significantly increased ERK, p38, and JNK phosphorylation in the SDH. Treatment with pyridoxamine significantly inhibited the increase in p-ERK in the SDH but did not affect the phosphorylation of JNK or p38 (Figure 7).

#### *Pyridoxamine reduced the AGE-LDL, ox-LDL, and IL-1 $\beta$ concentrations in the serum of diabetic rats*

AGE-LDL and ox-LDL interact with monocytes, macrophages, or endothelial cells, leading to oxidative and inflammatory responses.<sup>24–26</sup> We measured the AGE-LDL and ox-LDL concentrations in the serum of rats in the three groups and found that pyridoxamine suppressed the diabetes-induced increase in AGE-LDL and ox-LDL concentrations (Figure 8(a) and (b)).

IL-1 $\beta$  levels are elevated early in the course of type 1 diabetes (T1D), possibly contributing to T1D progression<sup>27</sup> and neuropathic pain.<sup>28</sup> Our results showed that

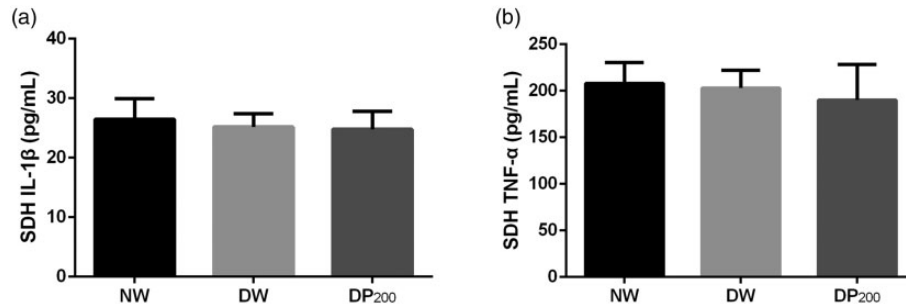


**Figure 4.** Concentrations of IL-1 $\beta$  and TNF- $\alpha$  in the SDH of rats in the three groups. (a) Concentrations of IL-1 $\beta$ . (b) Concentrations of TNF- $\alpha$ .  $N = 5$  per group.

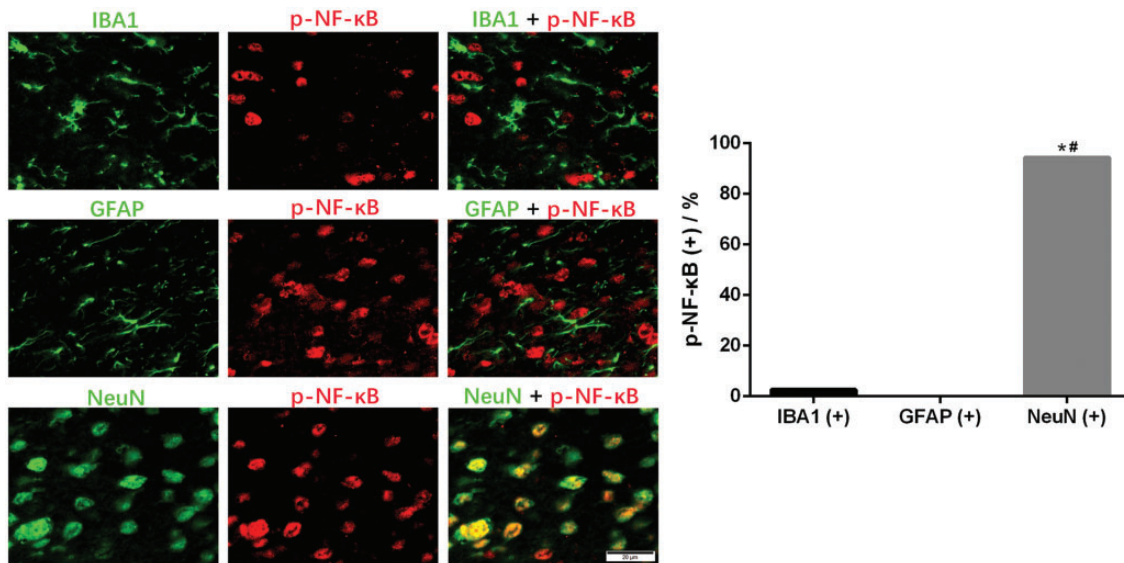


**Figure 5.** Distribution of p-NF- $\kappa$ B immunoreactivity in different cells in the SDH of diabetic rats. Representative images showing the double immunofluorescence staining of p-NF- $\kappa$ B (red) and IBA1 (green), GFAP (green) or NeuN (green). \* $P < 0.05$  vs. IBA1 coexpression, # $P < 0.05$  vs. GFAP coexpression.

IL-1 $\beta$  levels were elevated in the serum of rats in the DW group and that pyridoxamine inhibited this increase (Figure 8(c)).

## Discussion

Previous studies have reported that pyridoxamine may be useful in relieving the pain associated with spinal cord ischemia/reperfusion injury and osteoarthritis.<sup>12,13</sup> The objective of this study was to explore whether pyridoxamine, an inhibitor of protein glycation, could relieve DNP and systemic inflammation. To our knowledge, this study is the first to investigate the effect of pyridoxamine on DNP and to explore its underlying mechanisms. We demonstrated that pyridoxamine administration alleviated DNP at least partially by suppressing spinal RAGE-NF- $\kappa$ B/ERK signaling and ameliorated systemic inflammation by reducing the serum

concentrations of AGE-LDL, ox-LDL, and IL-1 $\beta$  in diabetic rats.

We used three dosages (100 mg/kg/day, 200 mg/kg/day, and 400 mg/kg/day) to explore the dose-dependent effects of pyridoxamine on DNP. Both the group that received 200 mg/kg/day and the group that received 400 mg/kg/day showed significant improvements in DNP; however, there were no significant differences in DNP between these two groups. We selected the pyridoxamine dosage of 200 mg/kg/day by referring to other published articles.<sup>29–31</sup> Furthermore, this dosage has been shown to significantly inhibit methylglyoxal-induced AGE formation and RAGE activation,<sup>10,32</sup> and a previous study demonstrated that RAGE activation is associated with mechanical allodynia.<sup>33</sup> Therefore, we chose 200 mg/kg/day as the optimal dosage of pyridoxamine.

Previous literature suggests that STZ-treated animals uniformly exhibit thermal hypersensitivity. We tried

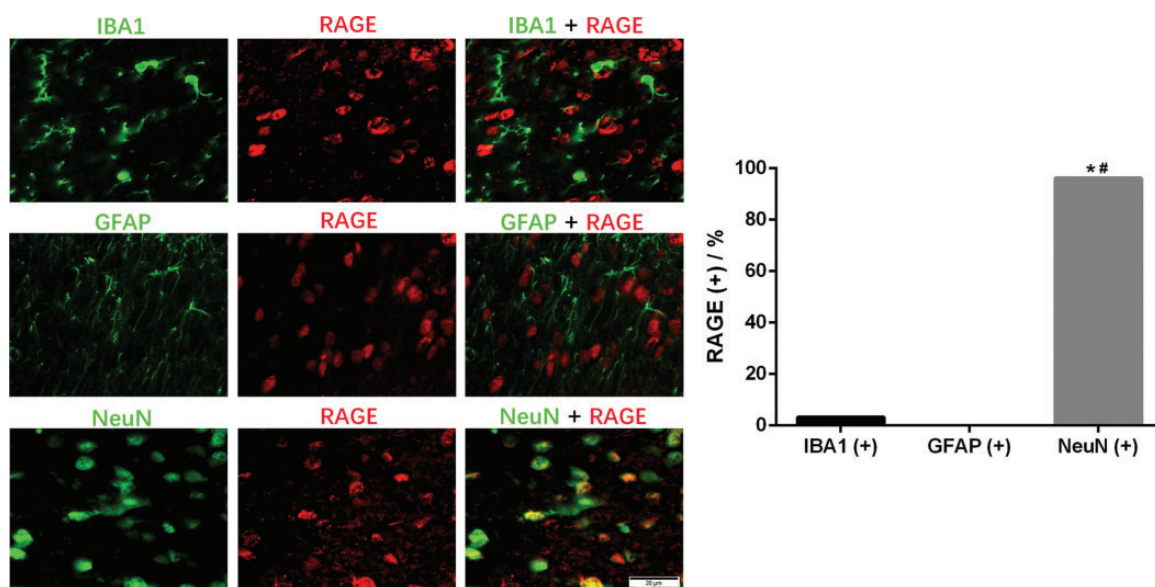


**Figure 6.** Distribution of RAGE immunoreactivity in different cells in the SDH of diabetic rats. Representative images showing double immunofluorescence staining of RAGE (red) and IBA1 (green), GFAP (green) or NeuN (green). \* $P < 0.05$  vs. IBA1 coexpression, # $P < 0.05$  vs. GFAP coexpression.

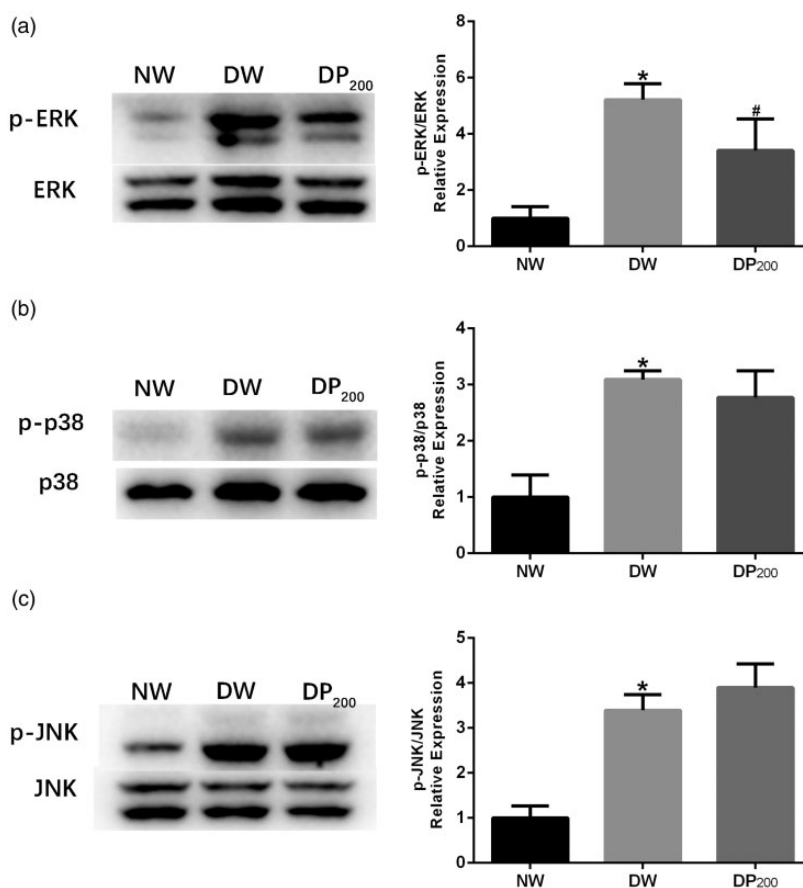


**Figure 7.** Expression of activated MAPKs in the SDH of rats in the three groups. (a) Representative western blots and statistical graphs showing the expression of p-ERK. (b) Representative western blots and statistical graphs showing the expression of p-p38. (c) Representative western blots and statistical graphs showing the expression of p-JNK. The band densities were normalized to those of the NW group. \* $P < 0.05$  vs. the NW group, # $P < 0.05$  vs. the DW group.  $N = 5$  per group.

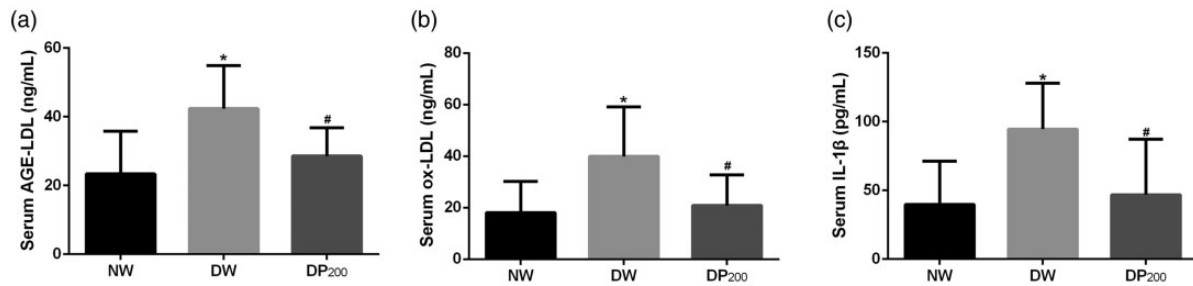


**Figure 8.** Concentrations of AGE-LDL, ox-LDL and IL-1 $\beta$  in the serum of rats in the three groups. (a) Concentrations of AGE-LDL. (b) Concentrations of ox-LDL. (c) Concentrations of IL-1 $\beta$ . \* $P < 0.05$  vs. the NW group, # $P < 0.05$  vs. the DW group.  $N = 8$  per group.

many methods, such as keeping the glass dry, using a fixed-power heat source, and testing when the rats were calm, to control the factors that may affect the PWTL results. However, we found no significant differences in the PWTL between the NW group and DW group. A PubMed search identified one other published article showing similar results.<sup>34</sup> Unknown factors may have resulted in the lack of differences in the PWTL between the NW and DW groups.

RAGE is a transmembrane receptor that belongs to the immunoglobulin gene superfamily. RAGE ligands include AGEs, high mobility group box 1 (HMGB1), S100/calgranulins, and  $\beta$ -amyloid, most of which can induce inflammatory and cell migration processes.<sup>35</sup> In addition to its classical effects, RAGE was found in recent studies to be associated with the occurrence of neuropathic pain. The levels of methylglyoxal, RAGE, and phosphorylated signal transducer and activator of transcription 3 (p-STAT3) were increased in the dorsal horn of bortezomib-treated rats, and these increases were accompanied by obvious mechanical allodynia. However, the intrathecal injection of a methylglyoxal scavenger, RAGE blocker or STAT3 inhibitor attenuated the bortezomib-induced mechanical allodynia and central sensitization.<sup>33</sup> Therefore, RAGE/STAT3 pathway activation plays important roles in bortezomib-induced mechanical allodynia. Another study indicated that RAGE mRNA expression in the lumbar dorsal root ganglion (DRG) was higher in injured rodents than in sham-injured rodents by postinjury day 28 and that RAGE antibody administration alleviated mechanical hyperalgesia.<sup>36</sup> Our results showed that RAGE expression was upregulated in the dorsal horn of rats 28 days after STZ injection and that pyridoxamine administration abrogated this change. We ascribed this phenomenon to the AGE-scavenging ability of pyridoxamine. Together, these results suggest that RAGE may play important roles in the mechanism underlying neuropathic pain.

Upon RAGE stimulation, the transcription factor NF- $\kappa$ B is activated,<sup>37,38</sup> and activated NF- $\kappa$ B can

upregulate the expression of RAGE via a positive feedback loop.<sup>20,39</sup> In this study, spinal RAGE expression was significantly higher in the DW group than in the NW group, and pyridoxamine administration inhibited spinal RAGE expression. NF- $\kappa$ B phosphorylation showed similar trends to RAGE expression. These results indicated that pyridoxamine inhibited the RAGE/NF- $\kappa$ B positive feedback loop, which was probably one of the mechanisms by which it alleviated DNP.

NF- $\kappa$ B activation in glial cells can induce inflammation and pain.<sup>40</sup> However, we found minimal levels of p-NF- $\kappa$ B in glial cells in the SDH of diabetic rats, and IL-1 $\beta$  and TNF- $\alpha$  levels were not increased in the SDH of diabetic rats. The western blotting and immunofluorescence staining results showed that diabetes increased the phosphorylation of NF- $\kappa$ B in neurons. Previous studies have reported that NF- $\kappa$ B activation in neurons is associated with neuroprotection<sup>41</sup> and with learning and memory.<sup>42</sup> One study reported that in DRG neurons, p65 can interact with the P2X3 receptor gene promoter and contribute to P2X3 receptor sensitization and diabetic pain hypersensitivity.<sup>43</sup> The NF- $\kappa$ B signaling pathway is also involved in the upregulation of Nav1.7 in DRG neurons in rats with diabetic neuropathy.<sup>44</sup> Therefore, the activation of NF- $\kappa$ B in spinal neurons may be associated with the upregulation of pain-related proteins; further investigation is necessary to interpret the meaning of this change.

MAPKs are a family of protein Ser/Thr kinases comprising ERK1/2, JNK1/2/3, p38 isoforms ( $\alpha$ ,  $\beta$ ,  $\gamma$ , and  $\delta$ ), and ERK5 and play important roles in proliferation, differentiation, apoptosis, immunity, and inflammation.<sup>45–47</sup> Several studies have indicated that the activation of MAPKs in the SDH contributes to DNP.<sup>23,48,49</sup> Certain drugs have been shown to relieve DNP by inhibiting the excessive activation of MAPKs.<sup>50,51</sup> Our results indicate that pyridoxamine suppresses ERK phosphorylation in the SDH, which is likely another mechanism by which pyridoxamine alleviates DNP. However, pyridoxamine did not affect phosphorylation of spinal p38 or JNK. In addition to MAPKs, the c-fos protein is also a



neural marker of DNP. Compared with control rats, STZ-injected rats presented significantly more c-fos-positive neurons.<sup>52</sup> We also examined whether pyridoxamine could affect the number of c-fos-positive neurons in the SDH of diabetic rats but found that pyridoxamine had no effect (data not shown). DNP is the result of multiple complex mechanisms, of which pyridoxamine affects some but not all.

RAGE signaling pathways and MAPK signaling are closely linked. ERK phosphorylation is an important step in the process of RAGE-mediated NF- $\kappa$ B activation,<sup>38,53</sup> p38 and JNK are phosphorylated when RAGE is activated.<sup>54</sup> Meng et al.<sup>55</sup> discovered that AGEs can activate the Raf/MEK/ERK signaling pathway through interactions with RAGE, induce autophagy, and regulate the proliferation and function of hFOB1.19 cells. In our research, diabetes significantly upregulated RAGE expression and ERK phosphorylation in the dorsal horn, and pyridoxamine inhibited this change. By referring to the abovementioned literature, we hypothesized that ERK phosphorylation occurs downstream of RAGE activation.

Under conditions of high plasma glucose levels, proteins can be modified by glucose and form AGEs.<sup>4</sup> LDL is susceptible to AGE modification, and AGE-LDL can induce proinflammatory cytokine production in endothelial cells and macrophages.<sup>56</sup> The results of the present study indicated that pyridoxamine can suppress the increase in AGE-LDL levels in the serum of diabetic rats. In addition, hyperglycemia can induce oxidative stress in diabetic subjects.<sup>57</sup> When lipoproteins are exposed to reactive oxygen species (ROS), amino acid residues on apolipoproteins may be oxidized and form ox-LDL.<sup>58</sup> Previous studies have shown that ox-LDL can stimulate mononuclear macrophages and activate the NLR family, pyrin domain-containing 3 (NLRP3) inflammasome, leading to the production of IL-1 $\beta$ .<sup>59,60</sup> In this study, pyridoxamine significantly reduced the serum concentrations of ox-LDL and IL-1 $\beta$  in diabetic rats. Systemic inflammation may contribute to the occurrence of pain.<sup>61</sup> The abovementioned results indicate that pyridoxamine can alleviate systemic inflammation in diabetic rats, potentially contributing to the alleviation of DNP.

Diabetic rats expressed elevated levels of IL-1 $\beta$  in the serum but not dorsal horn, which seems paradoxical. We analyzed this phenomenon and attributed it to three causes. First, proteins in the blood were directly exposed to high glucose conditions, and various kinds of proteins are more susceptible to advanced glycosylation in the blood than in the dorsal horn. Second, the number of inflammatory cells is higher in the blood than in the dorsal horn, a factor that could contribute to the levels of IL-1 $\beta$  in the serum. Third, RAGE and p-NF- $\kappa$ B were localized in neural cells but not glial cells in the dorsal

horn; therefore, no changes in IL-1 $\beta$  expression in the dorsal horn were found among the three groups.

In summary, pyridoxamine alleviated DNP by inhibiting the RAGE-NF- $\kappa$ B/ERK signaling pathway in the SDH; moreover, pyridoxamine suppressed the increase in AGE-LDL, ox-LDL, and IL-1 $\beta$  levels in the serum of diabetic rats, thus potentially contributing to the mitigation of systemic inflammation. Therefore, pyridoxamine is a promising drug for the clinical treatment of DNP. Further animal and clinical investigations need to be carried out to confirm the benefits of pyridoxamine.

### Author Contributions

XZ designed the study, conducted 70% of the experiments, analyzed the data, and drafted the manuscript. LX conducted 10% of the experiments. WC conducted 10% of the experiments. XY conducted 10% of the experiments. LS designed the study, analyzed the data, and revised the manuscript, and YH designed the study, analyzed the data, and revised the manuscript. All authors read and approved the final manuscript.

### Declaration of Conflicting Interests

The author(s) declared no potential conflicts of interest with respect to the research, authorship, and/or publication of this article.

### Funding

The author(s) disclosed receipt of the following financial support for the research, authorship, and/or publication of this article: This study was supported by a grant from the National Natural Science Foundation of China (No. 81671098).

### ORCID iDs

Xin Zhang  <https://orcid.org/0000-0001-8906-2117>

Le Shen  <https://orcid.org/0000-0002-2563-0012>

### References

1. Dermanovic Dobrota V, Hrabac P, Skegro D, Smiljanic R, Dobrota S, Prkacin I, Brkljacic N, Peros K, Tomic M, Lukinovic-Skudar V, Basic Kes V. The impact of neuropathic pain and other comorbidities on the quality of life in patients with diabetes. *Health Qual Life Outcomes* 2014; 12: 171–04.
2. Singleton JR, Smith AG. The diabetic neuropathies: practical and rational therapy. *Semin Neurol* 2012; 32: 196–203.
3. Schreiber AK, Nones CF, Reis RC, Chichorro JG, Cunha JM. Diabetic neuropathic pain: physiopathology and treatment. *World J Diabetes* 2015; 6: 432–444.
4. Virella G, Thorpe SR, Alderson NL, Stephan EM, Atchley D, Wagner F, Lopes-Virella MF, Group DER. Autoimmune response to advanced glycosylation end-products of human LDL. *J Lipid Res* 2003; 44: 487–493.

5. Ott C, Jacobs K, Haucke E, Navarrete Santos A, Grune T, Simm A. Role of advanced glycation end products in cellular signaling. *Redox Biol* 2014; 2: 411–429.
6. Brederson JD, Strakhova M, Mills C, Barlow E, Meyer A, Nimmrich V, Leddy M, Simler G, Schmidt M, Jarvis M, Lacy S. A monoclonal antibody against the receptor for advanced glycation end products attenuates inflammatory and neuropathic pain in the mouse. *Eur J Pain* 2016; 20: 607–614.
7. Iqbal Z, Azmi S, Yadav R, Ferdousi M, Kumar M, Cuthbertson DJ, Lim J, Malik RA, Alam U. Diabetic peripheral neuropathy: epidemiology, diagnosis, and pharmacotherapy. *Clin Ther* 2018; 40: 828–849.
8. Stover PJ, Field MS. Vitamin B-6. *Adv Nutr* 2015; 6: 132–133.
9. Abouzed TK, Munesue S, Harashima A, Masuo Y, Kato Y, Khailo K, Yamamoto H, Yamamoto Y. Preventive effect of salicylate and pyridoxamine on diabetic nephropathy. *J Diabetes Res* 2016; 2016: 1786789.
10. Almeida F, Santos-Silva D, Rodrigues T, Matafome P, Crisóstomo J, Sena C, Gonçalves L, Seica R. Pyridoxamine reverts methylglyoxal-induced impairment of survival pathways during heart ischemia. *Cardiovasc Ther* 2013; 31: e79–85.
11. Milne R, Brownstein S. Advanced glycation end products and diabetic retinopathy. *Amino Acids* 2013; 44: 1397–1407.
12. Yu CZ, Liu YP, Liu S, Yan M, Hu SJ, Song XJ. Systematic administration of B vitamins attenuates neuropathic hyperalgesia and reduces spinal neuron injury following temporary spinal cord ischaemia in rats. *Eur J Pain* 2014; 18: 76–85.
13. Garg S, Syngle A, Vohra K. Efficacy and tolerability of advanced glycation end-products inhibitor in osteoarthritis: a randomized, double-blind, placebo-controlled study. *Clin J Pain* 2013; 29: 717–724.
14. Zhong JM, Lu YC and Zhang J. Dexmedetomidine reduces diabetic neuropathy pain in rats through the Wnt 10a/beta-catenin signaling pathway. *Biomed Res Int* 2018; 2018: 9043628.
15. Teixeira JM, Dos Santos GG, Neves AF, Athie MCP, Bonet IJM, Nishijima CM, Farias FH, Figueiredo JG, Hernandez-Olmos V, Alshabani S, Tambeli CH, Müller CE, Parada CA. Diabetes-induced neuropathic mechanical hyperalgesia depends on P2X4 receptor activation in dorsal root ganglia. *Neuroscience* 2019; 398: 158–170.
16. Czerwińska ME, Gasińska E, Leśniak A, Krawczyk P, Kiss AK, Naruszewicz M, Bujalska-Zadrożny M. Inhibitory effect of Ligustrum vulgare leaf extract on the development of neuropathic pain in a streptozotocin-induced rat model of diabetes. *Phytomedicine* 2018; 49: 75–82.
17. Cheng YZ, Yang SL, Wang JY, Ye M, Zhuo XY, Wang LT, Chen H, Zhang H, Yang L. Irbesartan attenuates advanced glycation end products-mediated damage in diabetes-associated osteoporosis through the AGEs/RAGE pathway. *Life Sci* 2018; 205: 184–192.
18. Kumar Pasupulati A, Chitra PS, Reddy GB. Advanced glycation end products mediated cellular and molecular events in the pathology of diabetic nephropathy. *Biomol Concept* 2016; 7: 293–309.
19. Kay AM, Simpson CL, Stewart JA, Jr. The role of AGE/RAGE signaling in diabetes-mediated vascular calcification. *J Diabetes Res* 2016; 2016: 6809703–6809708.
20. Tobon-Velasco JC, Cuevas E, Torres-Ramos MA. Receptor for AGEs (RAGE) as mediator of NF- $\kappa$ B pathway activation in neuroinflammation and oxidative stress. *CNS Neurol Disord Drug Target* 2014; 13: 1615–1626.
21. Zhao M, Zhou A, Xu L, Zhang X. The role of TLR4-mediated PTEN/PI3K/AKT/NF- $\kappa$ B signaling pathway in neuroinflammation in hippocampal neurons. *Neuroscience* 2014; 269: 93–101.
22. Baker RG, Hayden MS, Ghosh S. NF- $\kappa$ B, inflammation, and metabolic disease. *Cell Metab* 2011; 13: 11–22.
23. Daulhac L, Mallet C, Courteix C, Etienne M, Duroux E, Privat AM, Eschalier A, Fialip J. Diabetes-induced mechanical hyperalgesia involves spinal mitogen-activated protein kinase activation in neurons and microglia via N-methyl-D-aspartate-dependent mechanisms. *Mol Pharmacol* 2006; 70: 1246–1254.
24. Toma L, Stancu CS, Sanda GM, Sima AV. Anti-oxidant and anti-inflammatory mechanisms of amlodipine action to improve endothelial cell dysfunction induced by irreversibly glycated LDL. *Biochem Biophys Res Commun* 2011; 411: 202–207.
25. Hong D, Bai YP, Gao HC, Wang X, Li LF, Zhang GG, Hu CP. Ox-LDL induces endothelial cell apoptosis via the LOX-1-dependent endoplasmic reticulum stress pathway. *Atherosclerosis* 2014; 235: 310–317.
26. Wang YC, Hu YW, Sha YH, Gao JJ, Ma X, Li SF, Zhao JY, Qiu YR, Lu JB, Huang C, Zhao JJ, Zheng L, Wang Q. Ox-LDL upregulates IL-6 expression by enhancing NF- $\kappa$ B in an IGF2-dependent manner in THP-1 macrophages. *Inflammation* 2015; 38: 2116–2123.
27. Grishman EK, White PC, Savani RC. Toll-like receptors, the NLRP3 inflammasome, and interleukin-1 $\beta$  in the development and progression of type 1 diabetes. *Pediatr Res* 2012; 71: 626–632.
28. Moalem G, Tracey DJ. Immune and inflammatory mechanisms in neuropathic pain. *Brain Res Rev* 2006; 51: 240–264.
29. Elseweidy MM, Elswefy SE, Younis NN, Zaghloul MS. Pyridoxamine, an inhibitor of protein glycation, in relation to microalbuminuria and proinflammatory cytokines in experimental diabetic nephropathy. *Exp Biol Med* 2013; 238: 881–888.
30. Brodeur MR, Bouvet C, Bouchard S, Moreau S, Leblond J, Deblois D, Moreau P. Reduction of advanced-glycation end products levels and inhibition of RAGE signaling decreases rat vascular calcification induced by diabetes. *PLoS One* 2014; 9: e85922.
31. Tanimoto M, Gohda T, Kaneko S, Hagiwara S, Murakoshi M, Aoki T, Yamada K, Ito T, Matsumoto M, Horikoshi S, Tomino Y. Effect of pyridoxamine (K-163), an inhibitor of advanced glycation end products, on

- type 2 diabetic nephropathy in KK-A(y)/Ta mice. *Metab Clin Exp* 2007; 56: 160–167.
32. Rodrigues T, Matafome P, Santos-Silva D, Sena C, Seica R. Reduction of methylglyoxal-induced glycation by pyridoxamine improves adipose tissue microvascular lesions. *J Diabetes Res* 2013; 2013: 690650.
  33. Wei JY, Liu CC, Ouyang HD, Ma C, Xie MX, Liu M, Lei WL, Ding HH, Wu SL, Xin WJ. Activation of RAGE/STAT3 pathway by methylglyoxal contributes to spinal central sensitization and persistent pain induced by bortezomib. *Exp Neurol* 2017; 296: 74–82.
  34. Daugherty DJ, Marquez A, Calcutt NA, Schubert D. A novel curcumin derivative for the treatment of diabetic neuropathy. *Neuropharmacology* 2018; 129: 26–35.
  35. Xie J, Méndez JD, Méndez-Valenzuela V, Aguilar-Hernández MM. Cellular signalling of the receptor for advanced glycation end products (RAGE). *Cell Signal* 2013; 25: 2185–2197.
  36. Allette YM, Due MR, Wilson SM, Feldman P, Ripsch MS, Khanna R, White FA. Identification of a functional interaction of HMGB1 with receptor for advanced glycation end-products in a model of neuropathic pain. *Brain Behav Immun* 2014; 42: 169–177.
  37. Litwinoff E, Hurtado Del Pozo C, Ramasamy R, Schmidt AM. Emerging targets for therapeutic development in diabetes and its complications: the RAGE signaling pathway. *Clin Pharmacol Ther* 2015; 98: 135–144.
  38. Rouhiainen A, Kuja-Panula J, Tumova S, Rauvala H. RAGE-mediated cell signaling. *Method Mol Biol* 2013; 963: 239–263.
  39. Li J and Schmidt AM. Characterization and functional analysis of the promoter of RAGE, the receptor for advanced glycation end products. *J Biol Chem* 1997; 272: 16498–16506.
  40. Kaltschmidt B and Kaltschmidt C. NF-kappaB in the nervous system. *Cold Spring Harb Perspect Biol* 2009; 1: a001271.
  41. Mattson MP, Goodman Y, Luo H, Fu W, Furukawa K. Activation of NF-kappaB protects hippocampal neurons against oxidative stress-induced apoptosis: evidence for induction of manganese superoxide dismutase and suppression of peroxynitrite production and protein tyrosine nitration. *J Neurosci Res* 1997; 49: 681–697.
  42. Meffert MK, Chang JM, Wiltgen BJ, Fanselow MS, Baltimore D. NF-kappa B functions in synaptic signaling and behavior. *Nat Neurosci* 2003; 6: 1072–1078.
  43. Zhang HH, Hu J, Zhou YL, Qin X, Song ZY, Yang PP, Hu S, Jiang X, Xu GY. Promoted interaction of nuclear factor-kappaB with demethylated purinergic P2X3 receptor gene contributes to neuropathic pain in rats with diabetes. *Diabetes* 2015; 64: 4272–4284.
  44. Huang Y, Zang Y, Zhou L, Gui W, Liu X, Zhong Y. The role of TNF-alpha/NF-kappa B pathway on the up-regulation of voltage-gated sodium channel Nav1.7 in DRG neurons of rats with diabetic neuropathy. *Neurochem Int* 2014; 75: 112–119.
  45. Kim EK, Choi EJ. Pathological roles of MAPK signaling pathways in human diseases. *Biochim Biophys Acta* 2010; 1802: 396–405.
  46. Peti W, Page R. Molecular basis of MAP kinase regulation. *Protein Sci* 2013; 22: 1698–1710.
  47. Arthur JS, Ley SC. Mitogen-activated protein kinases in innate immunity. *Nat Rev Immunol* 2013; 13: 679–692.
  48. Ogata Y, Nemoto W, Yamagata R, Nakagawasai O, Shimoyama S, Furukawa T, Ueno S, Tan-No K. Anti-hypersensitive effect of angiotensin (1–7) on streptozotocin-induced diabetic neuropathic pain in mice. *Eur J Pain* 2019; 23: 739–749.
  49. Daulhac L, Maffre V, Mallet C, Etienne M, Privat AM, Kowalski-Chauvel A, Seva C, Fialip J, Eschalier A. Phosphorylation of spinal N-methyl-d-aspartate receptor NR1 subunits by extracellular signal-regulated kinase in dorsal horn neurons and microglia contributes to diabetes-induced painful neuropathy. *Eur J Pain* 2011; 15: 169 e161–169 e112.
  50. Suzuki N, Hasegawa-Moriyama M, Takahashi Y, Kamikubo Y, Sakurai T, Inada E. Lidocaine attenuates the development of diabetic-induced tactile allodynia by inhibiting microglial activation. *Anesth Analg* 2011; 113: 941–946.
  51. Sun JS, Yang YJ, Zhang YZ, Huang W, Li ZS, Zhang Y. Minocycline attenuates pain by inhibiting spinal microglia activation in diabetic rats. *Mol Med Rep* 2015; 12: 2677–2682.
  52. Morgado C, Tavares I. C-fos expression at the spinal dorsal horn of streptozotocin-induced diabetic rats. *Diabetes Metab Res Rev* 2007; 23: 644–652.
  53. Lander HM, Tauras JM, Ogiste JS, Hori O, Moss RA, Schmidt AM. Activation of the receptor for advanced glycation end products triggers a p21(ras)-dependent mitogen-activated protein kinase pathway regulated by oxidant stress. *J Biol Chem* 1997; 272: 17810–17814.
  54. Taguchi A, Blood DC, del Toro G, Canet A, Lee DC, Qu W, Tanji N, Lu Y, Lalla E, Fu C, Hofmann MA, Kislinger T, Ingram M, Lu A, Tanaka H, Hori O, Ogawa S, Stern DM, Schmidt AM. Blockade of RAGE-amphoterin signaling suppresses tumour growth and metastases. *Nature* 2000; 405: 354–360.
  55. Meng HZ, Zhang WL, Liu F, Yang MW. Advanced glycation end products affect osteoblast proliferation and function by modulating autophagy via the receptor of advanced glycation end products/Raf protein/mitogen-activated protein kinase/extracellular signal-regulated kinase pathway. *J Biol Chem* 2015; 290: 28189–28199.
  56. Hodgkinson CP, Laxton RC, Patel K, Ye S. Advanced glycation end-product of low density lipoprotein activates the toll-like 4 receptor pathway implications for diabetic atherosclerosis. *Arterioscler Thromb Vasc Biol* 2008; 28: 2275–2281.
  57. Rains JL, Jain SK. Oxidative stress, insulin signaling, and diabetes. *Free Radic Biol Med* 2011; 50: 567–575.
  58. Arai H. Oxidative modification of lipoproteins. *Subcell Biochem* 2014; 77: 103–114.
  59. Li WL, Hua LG, Qu P, Yan WH, Ming C, Jun YD, Yuan LD, Nan N. NLRP3 inflammasome: a novel link between

- lipoproteins and atherosclerosis. *Arch Med Sci* 2016; 12: 950–958.
60. Jiang Y, Wang M, Huang K, Zhang Z, Shao N, Zhang Y, Wang W, Wang S. Oxidized low-density lipoprotein induces secretion of interleukin-1beta by macrophages via reactive oxygen species-dependent NLRP3 inflammasome activation. *Biochem Biophys Res Commun* 2012; 425: 121–126.
61. Blum E, Procacci P, Conte V, Hanani M. Systemic inflammation alters satellite glial cell function and structure. A possible contribution to pain. *Neuroscience* 2014; 274: 209–217.